The identity of the active site of oxalate decarboxylase and the importance of the stability of active-site lid conformations

Victoria J Just, Matthew R Burrell, Laura Bowater, Iain Mcrobbie, Clare Em Stevenson, David M Lawson, Stephen Bornemann

Biochemical Journal Immediate Publication. Published on 6 Aug 2007 as manuscript BJ20070708

The identity of the active site of oxalate decarboxylase and the importance of the stability of active site lid conformations

Victoria J. Just[1], Matthew R. Burrell, Laura Bowater, Iain McRobbie, Clare E. M. Stevenson, David M. Lawson and Stephen Bornemann[2]

Department of Biological Chemistry, John Innes Centre, Norwich Research Park, Norwich NR4 7UH, United Kingdom

Abbreviations used: ABTS, 2,2'-azinobis-(3-ethylbenzthiazoline-6-sulfonic acid).

[1] Current address: School of Medical Sciences, University Walk, Clifton, Bristol BS8 1TD, United Kingdom

[2] To whom correspondence should be addressed (stephen.bornemann@bbsrc.ac.uk; Tel. +44 1603 450741; Fax. +44 1603 450018).

The atomic co-ordinates have been deposited in the Protein Data Bank (http://www.rcsb.org) with accession number 2UY8 for R92A, 2UY9 for E162A, 2UYA for Δ162-3 and 2UYB for S161A.

Short title: Oxalate Decarboxylase

Biochemical Journal Immediate Publication. Published on 6 Aug 2007 as manuscript BJ20070708

Oxalate decarboxylase (EC 4.1.1.2) catalyses the conversion of oxalate to carbon dioxide and formate. It requires manganese and, uniquely, dioxygen for catalysis. It forms a homohexamer and each subunit contains two similar, but distinct, manganese sites termed sites 1 and 2. There is kinetic evidence that only site 1 is catalytically active and that site 2 is purely structural. However, the kinetics of enzymes with mutations in site 2 are often ambiguous and all mutant kinetics have been interpreted without structural information. Nine new site-directed mutants have been generated and four mutant crystal structures have now been solved. Most mutants targeted either the flexibility (T165P), favoured conformation (S161A, S164A, D297A or H299A) or presence (Δ162-3 or Δ162-4) of a lid associated with site 1. The kinetics of these mutants were consistent with only site 1 being catalytically active. This was particularly striking with D297A and H299A because they disrupted hydrogen bonds between the lid and a neighbouring subunit only when in the open conformation and were distant from site 2. These observations also provided the first evidence that the flexibility and stability of lid conformations are important in catalysis. The deletion of the lid to mimic the plant oxalate oxidase led to a loss of decarboxylase activity, but only a slight elevation in the oxalate oxidase side reaction, implying other changes are required to afford a reaction specificity switch. The four mutant crystal structures (R92A, E162A, Δ162-3 and S161A) strongly support the hypothesis that site 2 is purely structural.

Key words: oxalate decarboxylase, protein crystallography, *Bacillus subtilis*, protein engineering, manganese, oxalate oxidase.

INTRODUCTION

Oxalate decarboxylase (EC 4.1.1.2) catalyses the conversion of oxalate to carbon dioxide and formate in a reaction that involves the cleavage of a relatively inert C-C bond [1,2]. The enzyme, coded by the *oxdC* gene in *Bacillus subtilis,* is thought to be involved in the response to acid pH stress [3] and there has been a recent report that it is unexpectedly targeted to the cell wall [4]. It requires manganese II and, uniquely, dioxygen for catalysis [5]. A novel free radical catalytic cycle for this enzyme, based on the requirement for manganese and dioxygen, was proposed [5] and has since been elaborated with additional kinetic [6,7], spectroscopic [8,9], theoretical [10], mutagenic and structural [11,12] information (Scheme 1).

Properties shared with oxalate oxidases, including the requirement for manganese [13], shared membership of the cupin superfamily of proteins [14] and a predicted similar active site architecture [13,15] led to the proposal of a similar [13] but divergent [5] catalytic mechanism that has since had further input from structural [16,17], spectroscopic [18] and theoretical [19] studies (Scheme 1). When oxalate oxidase was first discovered to contain manganese, a catalytic cycle based on

manganese (III) and well known chemistry was considered unlikely since the resting state of the enzyme is predominantly in the manganese (II) oxidation state [13]. However, a recent study has provided evidence that the manganese (III) form of the plant enzyme could be the catalytically active form [20]. Whatever the case, a decarboxylase catalytic cycle based on manganese (III) would not require dioxygen in any obvious way, so would be unlikely as argued previously [5].

Both enzymes coordinate mononuclear manganese II ions with one Glu and three His residues [11,16], but the outcome of catalysis is expected to be dictated by the protonation of a formyl radical intermediate in only the decarboxylase reaction (perhaps together with the initial oxidation state of the manganese). Reaction specificity is not absolute because both enzymes have small amounts of the other respective activity [5,21]. These oxalate-degrading enzymes have potential commercial applications for diagnostics, gene therapy, bioremediation and crop improvement [22,23].

B. subtilis oxalate decarboxylase has two manganese binding sites (Fig. 1A [11,12]). Structural evidence that site 1 is the catalytic site includes the presence of formate bound to site 1 in one crystal structure [11] (together with spectroscopic support [9]), the presence of a suitable proton donor, Glu162, on a lid that can isolate site 1 from solvent [12] and the apparent solvent inaccessibility of site 2 in both known structures. Kinetic evidence includes the expected kinetic isotope effects and loss of activities when site 1 residues are mutated [7,12]. However, assumptions had to be made regarding the structural consequences of the mutations on activity. In addition, many site 2 mutants gave ambiguous results because they were severely compromised [11,12], precluding reliable kinetic isotope effect measurements and therefore the unambiguous assignment of site 2 as purely structural. Furthermore, the substitution of Glu162 was expected to result in an enzyme that had no decarboxylase activity but substantial oxidase activity [12]. Although a reaction specificity switch was reported with an E162Q mutant [7], it was modest (0.56 U mg^{-1} oxidase activity compared with a wild type activity decarboxylase of 79 U mg^{-1}), not observed in our laboratory [12] and not observed with any other substitution of Glu162. Finally, an approach that has not yet been explored is the mutation of the lid directed towards altering the flexibility and conformational stability of the active site lid.

This paper describes structural and kinetic evidence with site-directed mutants of *B. subtilis* oxalate decarboxylase that site 1 is indeed the sole catalytically active site, that the flexibility and stability of the conformations of the active site 1 lid are important in the catalytic cycle and that the conversion of a decarboxylase into an oxidase is not achievable by simply removing the lid with its Glu162 proton donor to mimic the plant oxalate oxidase.

EXPERIMENTAL

Materials

All materials and biochemicals were of the highest grade available and, unless stated otherwise, were purchased from Sigma-Aldrich. Protein concentration was determined using the Pierce Coomassie Plus-200 assay. Horse-radish peroxidase (HRP4C) was purchased from Biozyme Laboratories Ltd (Blaenavon, Gwent, Wales, UK). Dithiothreitol was obtained from Melford Laboratories Ltd (Suffolk, UK). Metal analysis was provided by Southern Science Laboratories (Lewes, Sussex, UK) using inductively coupled plasma emission spectroscopy of acid-digested samples. The metal content is quoted after the subtraction of control values obtained with buffer alone. Amino acid analysis of acid-digested protein using ion exchange ninhydrin chromatography was provided by the University of Cambridge Protein and Nucleic Acid Facility, UK.

Expression, purification and site-directed mutagenesis of His-tagged oxalate decarboxylase

The *oxdC* gene from *B. subtilis* strain 168 was inserted into the pET32a vector (Novagen) to give pLB36 as described previously [12]. This construct allowed expression of the *C*-terminally His-tagged protein in *E. coli* BL21(DE3). Site-directed mutagenesis of His-tagged oxalate decarboxylase was undertaken using the QuikChange Site-Directed Mutagenesis Kit (Stratagene) and the DNA sequence of each mutant was verified successfully. Cultures were grown and protein expression was induced with isopropyl-β-D-thiogalactopyranoside after heat shock-treatment at 42 °C and addition of $MnCl_2$ as described previously [12]. The heat shock-treatment was for either 2 or 20 min as indicated. Cells were harvested and broken to allow the purification of the protein using HiTrap Chelating HP columns (GE Healthcare) charged with $NiCl_2$ as described previously [12]. Active fractions were pooled and incubated for 1 h on ice with Chelex beads (Bio-Rad) to remove adventitiously bound divalent metal ions. The samples were then concentrated in the presence of 5 mM dithiothreitol and filtered (0.2 μm). Protein was further purified by gel filtration with a Superdex 200 HR 10/30 column (GE Healthcare) eluted with 20 mM Tris, pH 8.5, containing 0.5 M NaCl. Enzyme solutions were then concentrated to >10 mg ml^{-1} using Amicon Ultra filters (Millipore) and frozen in aliquots at -80 °C.

Oxalate decarboxylase assay

One unit of enzyme activity was defined as the conversion of 1 μmol of substrate to product per min. Oxalate decarboxylase activity at pH 4.0 was determined using a stopped assay at 26 ˚C, where the production of formate was coupled to the reduction of NAD by formate dehydrogenase as previously described [5]. Unless otherwise stated, the oxalate decarboxylase reaction mixtures contained 1-150 mM potassium oxalate, air saturated 100 mM sodium citrate pH 4.0, 300 μM *o*-

phenylenediamine, 10 μM bovine serum albumin and enzyme (up to 1.5 mg ml^{-1}) and were incubated for 10 min. Michaelis-Menten constants and their standard errors were estimated by fitting data using the Pharmacology-Simple Ligand Binding-One Site Saturation option in SigmaPlot v8.0.

Oxalate oxidase and dye oxidation assays

Oxalate oxidase activity was determined spectrophotometrically at 23 ˚C using a continuous assay, where the production of hydrogen peroxide was coupled to the single electron oxidation of 2,2'-azinobis-(3-ethylbenzthiazoline-6-sulfonic acid) (ABTS) using horse-radish peroxidase as described previously [13]. Reaction mixtures contained 50 mM sodium citrate buffer pH 4.0, horse-radish peroxidase (25 units; as defined by supplier), 5 mM ABTS, 20 mM potassium oxalate and enzyme (up to 0.02 mg ml^{-1}). Assays were performed in at least duplicate. In order to distinguish between oxalate oxidase (i.e. hydrogen peroxide production) and direct oxalate-dependent single-electron dye oxidation activities of the enzyme, controls without peroxidase were necessary.

X-ray crystallography

Protein samples were supplemented with 5 mM dithiothreitol and 0.5 mM $MnCl_2$ and filtered (0.2 μm) before crystallisation using the hanging drop vapour diffusion method at 18 °C. The mutant enzymes generally crystallised with 8-15% polyethylene glycol 8,000, 0.1 M Tris, pH 8.5, with 0-15% xylitol. The conditions for each mutant were then optimised (see online data). The crystals were cryoprotected using crystallisation solution containing 25% glycerol in place of an equivalent volume of buffer, and flash-cooled to 100 K for data collection. Diffraction data were collected in-house using a Mar 345-image plate detector (X-ray Research) mounted on a Rigaku RU-H3RHB rotating anode X-ray generator (operated at 50 kV and 100 mA) fitted with Osmic confocal optics and a copper target (Cu Kα; λ = 1.542 Å). Additional X-ray data were recorded at the ESRF in Grenoble (France) on beamline ID14-2 (λ = 0.933 Å) using an ADSC Quantum 4 CCD. The diffraction data were integrated using MOSFLM [24] and scaled with SCALA [25]. All other downstream data processing and statistical analyses were carried out using programs from the CCP4 software suite [26]. The crystals were essentially isomorphous with those previously obtained [12]. They all belonged to space group *R*32 with approximate cell parameters of a = b = 155 and c = 122 Å and contained a single monomer per asymmetric unit, giving an estimated solvent content of 62% [27]. Details of the data collection and processing statistics are summarised in Table 1. The initial coordinate sets and starting phases were obtained by rigid body refinement of the 2.0 Å resolution closed structure [12] (Protein Data Bank entry code 1UW8) against the new datasets using the program REFMAC5 [28]. Model building was performed by interactive computer

graphics using the programs O [29] and COOT [30] with reference to SIGMAA-weighted [31] $2mF_{obs} - dF_{calc}$ and $mF_{obs} - dF_{calc}$ Fourier electron density maps. Positional and thermal parameters of the model were subsequently refined using REFMAC5. The electron density maps confirmed the presence of each expected mutation. A summary of the model contents and geometrical parameters of the final structures is given in Table 1. To compare the structures of the two manganese binding sites, each were independently superposed on the closed structure on the basis of the Cα positions of the four amino acids providing ligands to the manganese.

EPR spectroscopy

X-band EPR spectroscopy was performed on a Bruker ELEXSYS 500 spectrometer with an ER049X SuperX microwave bridge and a shq cavity. Low temperature experiments were performed using an Oxford Instruments ESR-900 cryostat and ITC3 temperature controller. Conditions were adjusted to ensure non-saturation of signals. Spectra were obtained with a microwave frequency of 9 GHz and power of 2 mW at 30 K.

Molecular modelling

The dominant conformation of the lid of the T165P mutant was estimated using Swiss-PDBViewer v3.6b3 [32]. The feasibility of disulphide bond formation in double mutants of oxalate decarboxylase was modelled on the basis of the open and closed structures (Protein Data Bank entry codes 1J58 and 1UW8) [11,12] using this application.

RESULTS AND DISCUSSION

Structure of and ligand binding to the R92A mutant

We have previously shown that the R92A mutant lacks both oxalate decarboxylase and oxalate oxidase activities (Table 2 [12]). This had been rationalised as the requirement of Arg92 to bind the substrate and/or stabilise catalytic intermediates [12] as supported by recent kinetic isotope effect measurements [7]. It was important to obtain structural information in order to rule out any unexpected consequences of this mutation, especially at site 2. The crystal structure of the R92A mutant was obtained at 2.8 Å resolution (Fig. 2). The conformation of the main chain at amino acid 92 was unchanged. At least one water molecule occupied the space in the mutant structure that the guanidinium group of the Arg92 side chain took up in the wild type structures [11,12]. The site 1 lid was in a conformation closely similar to that of the open structure. This might have been due to the inability of Glu162 to form a hydrogen bond with Arg92 in the closed conformation of this mutant. Formate, which was added to the crystallisation solution, was not observed bound to the site 1 manganese ion but two water molecules were. The manganese ion was slightly displaced (~0.5 Å

compared with the closed and open wild type structures) towards the core of the protein. This was accompanied by a shift in the position of His97, including its main chain atoms, together with a 180º flip of the imidazole ring to maintain its coordination to the metal ion. Incidentally, this flipped conformation resembles that of the equivalent residue in the plant oxalate oxidase structure [16], where there is an Asn in the equivalent position of Arg92. Site 2 (Fig. 1B) was indistinguishable from that of the wild type closed structure [12].

The lack of activity of this mutant could have been due to a lack of turnover or simply the lack of binding of oxalate. Indeed, formate was not bound in the crystal of the mutant despite its addition to the crystallisation conditions and its presence in the wild type open structure [11]. However, the manganese EPR spectrum of the anaerobic enzyme in frozen solution changed in the presence of either formate or oxalate (Fig. 3). The spectral changes were qualitatively similar to those observed previously with the wild type enzyme [33] indicating similar modes of binding to site 1 despite the mutation. It would therefore appear that a lack of catalysis rather than a lack of binding was primarily responsible for the poor activity of this mutant. These results are consistent with site 1 being the only catalytic site and that Arg92 is essential for activity.

Structure of the E162A mutant

We have previously shown that the E162A mutant possesses no oxalate decarboxylase activity but retains most of its oxalate oxidase side activity (Table 2 [12]). It has been suggested that this provides evidence that Glu162 is the proton donor required to complete the decarboxylase reaction [12]. Again, this was on the assumption that the structure of site 2 was unchanged. The structure of the E162A mutant was determined to 3.1 Å resolution. In this case, the lid was in an essentially closed conformation (Fig. 2), perhaps because of the loss of extensive hydrogen bonding interactions in the open state involving Glu162 [11]. Unfortunately the data did not permit solvent or other ligands to be modelled with confidence; although we assume that there was no formate bound to site 1, as was the case with the closed form of the wild type enzyme [12]. No changes were apparent in site 2 (Fig. 1B), consistent with Glu162 being the proton donor.

We have previously shown that the E162Q mutant exhibits only 1% the decarboxylase activity of the wild type enzyme (Table 2 [12]). A recent report presented evidence for an additional modest increase in oxalate oxidase activity [7], when the enzyme was purified and activity was determined using alternative methods. We have obtained crystals of this mutant that were isomorphous with those of the wild type with cell parameters of a = b = 155.1 and c = 121.3 Å, indicating that the overall fold and oligomerisation state of the protein were unchanged. However, the crystals diffracted weakly, yielding a very poor data set to ~4 Å resolution (data not shown), such that the structure could not be determined with confidence.

Additional mutations of Glu162 or Glu333

We have previously shown that the substitution of Glu162 near site 1 with either Ala or Gln results in a dramatic lowering of decarboxylase V_{max} (Table 2 [12]). The equivalent mutations in site 2 of Glu333 also lowered the V_{max} substantially (Table 2 [12]). What was not clear however, was the reason why such mutations at site 2 should have such a significant effect if site 1 were responsible for decarboxylase activity.

In order to probe this further, each of these Glu residues was substituted by Asp. These mutants (Table 3) were expressed in *E. coli* using a heat shock for 20 min at 42 °C prior to induction (similar to a method reported by others [6]), rather than 2 min as had been used for the enzymes described in Table 2 [12]. This new protocol gave a wild type enzyme preparation with an improved specific activity. This new protocol was therefore used for all new mutants (Table 3) unless indicated otherwise.

The E162D mutant retained 29% the decarboxylase activity. Such changes were not unexpected because the Asp side chain could still function as the proton donor in the decarboxylase reaction, but less efficiently due to its inevitably different position relative to the active site. It was surprising that the E333D mutant was much more severely affected, with the retention only 1% of the V_{max} of the wild type enzyme, consistent with a recent report [7]. It must be noted however, that this mutant gave two orders of magnitude lower yields of purified soluble protein compared with the wild type and was the only mutant to do so in this laboratory. This implied that the kinetic data might not have reflected the true catalytic properties of this mutant. Indeed, gel filtration and dynamic light scattering revealed an unusual ability of this mutant to exist as a trimer and an aggregate in addition to the normal hexamer. The trimer exhibited a specific activity of about half that of the hexamer. A recent report described a similar oligomeric distribution with this mutant and its tendency to lose manganese [7]. It would therefore appear that this residue has an important role, either directly or indirectly, in both oligomerisation and metal affinity. One possible reason is that a Glu333 carboxylate O atom in the wild type enzyme is within ~2.8 Å of the Nε atom of Arg270. This close interaction would presumably not be possible in the E333D mutant and such a buried and unfulfilled salt bridge could be disruptive.

Deletion of the lid

As described above, the substitution of the Glu162 residue in the oxalate decarboxylase site 1 lid with Ala or Gln dramatically lowers activity (Table 2 [12]). If this were due to the loss of the active site proton donor for the decarboxylase reaction, one might have expected that the enzyme would have undergone a complete switch to an oxalate oxidase, but it had not. When the structures of the

bacterial oxalate decarboxylase and plant oxalate oxidase were superposed, it was apparent that the site 1 lid, including its Glu residue, was absent in the oxidase [12]. Such a structural alignment indicated that the loop is two or maybe three amino acids shorter in the oxidase, preventing formation of the lid (Fig. 1A and 2 and online data).

In order to test whether the absence of the lid was a prerequisite for oxidase activity, as well as the loss of the Glu residue, a deletion mutant was prepared (using the short heat shock protocol in this case). The loss of the Glu162 and Asn163 residues in the Δ162-3 mutant resulted in a decarboxylase V_{max} of 1% and k_{cat}/K_m of 7% as expected (Table 2). Its oxidase activity was increased ~2.5-fold. While this approach was somewhat successful, the oxalate oxidase V_{max} of the mutant was still two orders of magnitude less than that of the plant oxidase [13].

The structure of this Δ162-3 mutant was solved to 2.0 Å. The lid took up a well ordered conformation and, due to its small size, site 1 was relatively open as expected (Fig. 2). Electron density between one of the water molecules bound to the site 1 manganese ion and Arg92 was best modelled by the introduction of a chloride ion. This site is occupied by a carboxyl O atom of either formate in the open structure [11] or Glu162 in the closed structure [12]. This illustrated the propensity for this site to bind negative charges. Halide ions have been reported to bind to the manganese ion of oxalate oxidase according to EPR spectroscopy [18]. However, in this case it was suggested that chloride displaced the water molecules directly bound to the metal ion, which was not the situation in the decarboxylase mutant structure. The site 2 structure was again unchanged (Fig. 1B).

It was apparent from the comparison of this mutant structure with that of the plant oxalate oxidase [16] that the deletion of two residues from the lid was not enough to remove it completely and that a third amino acid deletion would be required to further open the entrance to site 1. On this basis, a third residue, Ser164, was also deleted to give the Δ162-4 mutant, in order to make sure that the lid was completely removed. This mutant exhibited no detectable decarboxylase activity but a ~3-fold increase in oxalate oxidase activity compared with wild type (Table 3). Therefore the removal of a third residue enhanced the effect of removing the first two, but did not result in the complete conversion of a decarboxylase into an efficient oxalate oxidase. Its oxidase activity was also less than that reported for E162Q by others [7].

It is clear that additional mutations are required to afford an efficient conversion by stabilising intermediates associated with the oxidase catalytic cycle. This could include changing the lining of the site 1 active site to resemble more the plant oxidase [17] or perhaps making multiple changes around site 1 to resemble the predicted structure of a fungal oxidase [21]. Such changes could influence factors such as the affinity of the enzyme for oxygen and perhaps the reduction potential of the manganese ion.

Mutation of the lid affecting flexibility

If site 1 were the only active site, mutations of the site 1 lid, other than of Glu162, would be expected to interfere with its flexibility and ability to open and close thus impairing substrate entry, positioning of Glu162 for catalysis, product release and therefore enzyme activity. One way in which the lid flexibility could be limited would be to introduce a Pro residue in place of one of the amino acids that undergoes the greatest backbone conformational changes [12]. Molecular modelling identified T165P as being the most promising mutation that would least disrupt the lid while at the same time strongly favour the closed conformation. This mutant's V_{max} and k_{cat}/K_m were very low (3 and 1%, respectively), as expected (Table 3).

Mutations of the lid affecting hydrogen bonding in either the closed or open conformations

Of interest was the effect of preventing the formation of hydrogen bonds associated with the lid in one or other of its conformations. The Ser161 side chain forms hydrogen bonds to the Thr44 side chain, Glu67 side chain and Asn163 main chain NH in the closed form [12] but only a water molecule in the open form [11]. One might expect therefore that the closed form of a S161A mutant might be destabilised. The S161A mutant retained 15% of its decarboxylase V_{max} (Table 3), indicating that such a modest mutation near site 1 did have a detrimental effect on catalytic activity. Furthermore, the affinity for oxalate was affected more than in any other mutant tested, giving a 10-fold increase in K_m and a k_{cat}/K_m of only 1%.

The structure of the S161A mutant was solved to 2.1 Å resolution. The lid adopted an essentially closed conformation (Fig. 2). This mutant was designed with the destabilisation of the closed conformation in mind, so the structure was somewhat surprising. Formate was clearly bound to site 1 in a manner previously seen in the open conformation only [11]; noting that in neither case was formate deliberately added to the crystallisation conditions. The side chain of Glu162 was within hydrogen bonding distance of the formate and Tyr200. These interactions perhaps accounted for the lid being closed. Indeed, this is the first known closed structure with formate bound.

These results may give an insight into the structure of the enzyme when it is poised to protonate the proposed formyl radical intermediate. Glu162 is well positioned to act as the proton donor. However, in this chemical step, the formyl radical would be expected to be in an altered conformation after radical decarboxylation allowing the proton to be transferred to the formyl carbon atom. Interestingly, the observed formate conformation could resemble that required for the formyl radical of the oxalate oxidase reaction to either form percarbonate or facilitate electron transfer with manganese-bound oxygen.

There was a water molecule within hydrogen bonding distance of the formate, Glu162 and Thr165 in the mutant structure. The side chain of Thr165 was in the same conformation as in the open wild type structure but flipped relative to that in the closed structure (not shown). The side chain conformation in the mutant structure of an adjacent residue, Gln167, was also more similar to that of the open structure (not shown). The position taken up by the water molecule is unoccupied in all other structures. One can speculate that this position could be occupied by carbon dioxide after the decarboxylation step and that the Thr165 side chain could flip to modulate the hydrophobicity of this site. The site 2 structure was unchanged (Fig. 1B).

The Ser164 residue of the wild type enzyme makes hydrogen bonds to the Glu99 side chain, the Ser161 main chain NH and a water molecule in the open form [11] and none in the closed form [12]. It would therefore be expected that the open form of the lid of a S164A mutant would be destabilised. Interestingly the V_{max} of this mutant was similar to that of the S161A mutant giving 15% of that of the wild type enzyme (Table 3). However, the K_m of this mutant was less affected giving a k_{cat}/K_m of 3%. The oxalate oxidase activities of the S161A and S164A mutants were much lower than that of the wild type, indicating that the site 1 lid had some influence on this side reaction too.

Mutations near the lid affecting hydrogen bonding in the open conformation

In order to better assess whether the lid and the stability of its open conformation are important for catalysis and that site 1 is the only catalytic site, mutations were considered that would have more subtle effects. The Glu162 side chain makes hydrogen bonds to the Asp297 side chain, the His299 side chain, the Thr44 side chain and Thr44 main chain NH when in the open form [11]. These three residues are present on the surface of neighbouring subunits, are remote from site 2 and, in the case of the first two, are not involved in interactions with the lid when in the closed form. It was therefore of interest to establish whether mutations of the first two residues would affect catalytic activity.

Both the D297A and H299A mutants had their decarboxylase V_{max} lowered by half with little change in their K_m for oxalate (Table 3). This provides compelling evidence that only site 1 is catalytically active. Quite why the D297A mutant exhibited one of the highest oxalate oxidase activities of any of the mutants tested is not clear, but its absolute value is nevertheless small.

Manganese content of mutant enzymes

Some of the oxalate decarboxylase mutant enzymes were selected for metal analysis using inductively coupled plasma emission spectroscopy (Table 4). What is immediately apparent is that none of the enzymes, including the wild type, contained the theoretical maximum of two atoms of

manganese per subunit. While the method we used for metal analysis is generally considered to be reliable, protein assays are not necessarily so. We compared the results from the protein assay based on dye-binding with amino acid analysis, which is generally considered to be a reliable method for protein determination, and found that they gave indistinguishable results. Therefore, the metal contents of enzymes presented in Table 4 can be considered to be good estimates.

There was no correlation between the manganese content of the enzymes and their decarboxylase V_{max} (Table 4). For example, although the mutants with the lowest manganese content (R92A and E333Q) possessed no decarboxylase activity, the mutant with the second highest manganese content (E162A) also had no decarboxylase activity. In addition, the mutant with a manganese content closest to two atoms per subunit (E162Q) had only 1% the decarboxylase V_{max} of the wild type and the most active mutant tested (E333A) had a lower manganese content than the wild-type.

The fact that there were essentially full manganese occupancies for both binding sites in all of the crystal structures (as estimated from temperature factors) shows that the crystals represented a subpopulation of the enzymes in solution. This implies that the protein without full manganese occupancy exhibited conformational disorder that disfavoured crystallisation.

Oxalate-dependent dye oxidation

Oxalate decarboxylase is known to catalyse the oxalate-dependent oxidation of dyes [5]. The exact chemical details of this reaction are not known. There was a similar increase in the decarboxylase V_{max} and the dye oxidation rate when the wild type enzyme was prepared with the longer heat shock protocol (Tables II and III). The rate of dye oxidation catalysed by the mutants varied between 7 and 233% compared with the wild type enzyme. There was no obvious correlation between the rate of this side reaction and either the rate of oxalate decarboxylation or oxalate oxidation with the mutants, but the error in determining such small rates might have obscured any correlation.

Summary of structural evidence for the identity of the catalytic site

Evidence for site 1 being the sole or dominant active site has previously been presented on the basis of the kinetics of a limited number of site specific mutants [12], but assumptions were made regarding their structures. We have now solved the structures of two of these mutants. We have also generated and kinetically characterised another nine mutants and solved the structures of two of them. The structural changes in site 1 of the mutants are consistent with their kinetic properties and the hypothesis that site 1 is the main or sole catalytic centre. In none of the crystal structures described was site 2 in any obvious way disrupted.

There are now a total of six structures of oxalate decarboxylase known. Of these, 2 have formate bound despite formate not being added to the crystallisation conditions. In each case the formate was bound to the site 1 manganese *trans* to the His140 ligand. The equivalent coordination site in the plant oxalate oxidase is known to be capable of binding the oxalate analogue, glycolate [17]. The presence of the product of the decarboxylase reaction, formate, exclusively in site 1 in two decarboxylase structures adds more weight to the argument that site 1 is the only catalytically active site.

Summary of additional kinetic evidence for the identity of the catalytic site and the importance of lid flexibility and conformational stability in the catalytic cycle

Several mutagenic approaches were taken to lend further support for site 1 being the catalytically active site. These included deletion of much of the lid, the restriction of lid flexibility and the disruption of hydrogen bonding between the lid and the rest of the protein. All of these mutants led to a loss of decarboxylase activity. In a separate set of experiments (data not shown), preliminary kinetic data with the mutants T44C.S161C and S161C.S164C indicated that it was possible to turn decarboxylase activity on and off by preventing or promoting disulfide formation. Disulfide formation would lead to the lid being locked in the closed conformation according to molecular modelling. Further work on such a redox-controlled switch will be required to develop this approach.

The effect of the mutations of the lid on V_{max} are generally easy to rationalise. However, the effects on K_m are not so easy to explain. The affinity for oxalate was decreased in most of the new mutants generated. The only side chains of the lid to line site 1 are those of Glu162 and Thr165 and that is when the lid is closed. The implication is that the lid has an important role in substrate affinity, through gating access to site 1 as well as its precise conformation when closed.

The most compelling kinetic evidence that site 1 is most likely the only catalytically active site came from the significant lowering of activity when hydrogen bonds between the open lid and the rest of the protein were disrupted. This also suggest that the open conformation is accessed during the catalytic cycle and that the conformational stability and/or movement of the lid can limit the rate of reaction. It is interesting to note that the Gibbs energy of activation associated with the wild type V_{max} (Table 3) is 62.4 kJ mol^{-1} while that of the above mutants is 64.2 kJ mol^{-1}. Thus the $\Delta\Delta G^{\ddagger}$ is 1.7 kJ mol^{-1}, which is comparable to the typical strength of a hydrogen bond of 2-6 kJ mol^{-1}; noting that no implication is made that hydrogen bonds associated with these residues are directly involved with the rate limiting transition state. Nevertheless, there is clearly a fine balance between the stabilities of the open and closed conformations to allow efficient catalysis.

The lid has to open to allow access of the substrates to site 1 and we have presented the first evidence that the stability of the open conformation is indeed important in catalysis. Partial closure would then be required if Glu162 were the base that abstracted the proton from the bound oxalate when the oxalate radical forms. It certainly would have to close in order for Glu162 to protonate the formyl radical intermediate. The lid would then have to open in order to release the products. Why the lid should isolate the catalytic site from solvent when closed is not clear. It could be that catalysis is more efficient within the closed protein environment for electrostatic reasons, that the free radical chemistry might be interrupted if other small molecules, such as redox active dyes like ABTS, have access to reactive catalytic intermediates, that it is important to avoid non-specific protonation of dioxygen when bound to the manganese ion or that the reduction potential of the manganese ion requires modulation during the cycle. However, the plant oxidase does not appear to require a lid to function [16], so perhaps the lid is only essential for the decarboxylase reaction. Further work is required to address these issues.

We thank Sascha Keller for assistance with crystallographic data collection, Shirley Fairhurst for electron paramagnetic spectroscopy and Peter Sharratt for the amino acid analysis. This work was supported by the Biotechnology and Biological Sciences Research Council with a grant (C18140 to V.J.J.), a Committee Studentship (to M.R.B.) and a Core Strategic Grant to the John Innes Centre. This paper is dedicated to Professor David J. Lowe on the occasion of his retirement.

REFERENCES

1 Begley, T. P. and Ealick, S. E. (2004) Enzymatic reactions involving novel mechanisms of carbanion stabilization. Curr. Opin. Chem. Biol. **8**, 508-515

2 Svedruzic, D., Jonsson, S., Toyota, C. G., Reinhardt, L. A., Ricagno, S., Linqvist, Y. and Richards, N. G. J. (2005) The enzymes of oxalate metabolism: unexpected structures and mechanisms. Arch. Biochem. Biophys. **433**, 176-192

3 Tanner, A. and Bornemann, S. (2000) *Bacillus subtilis* YvrK is an acid-induced oxalate decarboxylase. J. Bacteriol. **182**, 5271-5273

4 Antelmann, H., Towe, S., Albrecht, D. and Hecker, M. (2007) The phosphorus source phytate changes the composition of the cell wall proteome in *Bacillus subtilis*. J. Proteome Res. **6**, 897-903

5 Tanner, A., Bowater, L., Fairhurst, S. A. and Bornemann, S. (2001) Oxalate decarboxylase requires manganese and dioxygen for activity - overexpression and characterization of *Bacillus subtilis* YvrK and YoaN. J. Biol. Chem. **276**, 43627-43634

6 Reinhardt, L. A., Svedruzic, D., Chang, C. H., Cleland, W. W. and Richards, N. G. J. (2003) Heavy atom isotope effects on the reaction catalyzed by the oxalate decarboxylase from *Bacillus Subtilis*. J. Am. Chem. Soc. **125**, 1244-1252

7 Svedruzic, D., Liu, Y., Reinhardt, L. A., Wroclawska, E., Cleland, W. W. and Richards, N. G. J. (2007) Investigating the roles of putative active site residues in the oxalate decarboxylase from *Bacillus subtilis*. Arch. Biochem. Biophys., in press

8 Chang, C. H., Svedruzic, D., Ozarowski, A., Walker, L., Yeagle, G., Britt, R. D., Angerhofer, A. and Richards, N. G. J. (2004) EPR spectroscopic characterization of the manganese center and a free radical in the oxalate decarboxylase reaction - identification of a tyrosyl radical during turnover. J. Biol. Chem. **279**, 52840-52849

9 Angerhofer, A., Moomaw, E. W., Garcia-Rubio, I., Ozarowski, A., Krzystek, J., Weber, R. T. and Richards, N. G. J. (2007) Multifrequency EPR studies on the Mn(II) centers of oxalate decarboxylase. J. Phys. Chem. B **111**, 5043-5046

10 Chang, C. H. and Richards, N. G. J. (2005) Intrinsic carbon-carbon bond reactivity at the manganese center of oxalate decarboxylase from density functional theory. J. Chem. Theory Comput. **1**, 994-1007

11 Anand, R., Dorrestein, P. C., Kinsland, C., Begley, T. P. and Ealick, S. E. (2002) Structure of oxalate decarboxylase from *Bacillus subtilis* at 1.75 Å resolution. Biochemistry **41**, 7659-7669

12 Just, V. J., Stevenson, C. E. M., Bowater, L., Tanner, A., Lawson, D. M. and Bornemann, S. (2004) A closed conformation of *Bacillus subtilis* oxalate decarboxylase OxdC provides evidence for the true identity of the active site. J. Biol. Chem. **279**, 19867-19874

13 Requena, L. and Bornemann, S. (1999) Barley (*Hordeum vulgare*) oxalate oxidase is a manganese-containing enzyme. Biochem. J. **343**, 185-190

14 Dunwell, J. M. and Gane, P. J. (1998) Microbial relatives of seed storage proteins: Conservation of motifs in a functionally diverse superfamily of enzymes. J. Mol. Evolution **46**, 147-154

15 Gane, P. J., Dunwell, J. M. and Warwicker, J. (1998) Modeling based on the structure of vicilins predicts a histidine cluster in the active site of oxalate oxidase. J. Mol. Evolution **46**, 488-493

16 Woo, E. J., Dunwell, J. M., Goodenough, P. W., Marvier, A. C. and Pickersgill, R. W. (2000) Germin is a manganese containing homohexamer with oxalate oxidase and superoxide dismutase activities. Nature Struct. Biol. **7**, 1036-1040

17 Opaleye, O., Rose, R. S., Whittaker, M. M., Woo, E. J., Whittaker, J. W. and Pickersgill, R. W. (2006) Structural and spectroscopic studies shed light on the mechanism of oxalate oxidase. J. Biol. Chem. **281**, 6428-6433

18 Whittaker, M. M. and Whittaker, J. W. (2002) Characterization of recombinant barley oxalate oxidase expressed by *Pichia pastoris*. J. Biol. Inorg. Chem. **7**, 136-145

19 Borowski, T., Bassan, A., Richards, N. G. J. and Siegbahn, P. E. M. (2005) Catalytic reaction mechanism of oxalate oxidase (germin). A hybrid DFT study. J. Chem. Theory Comput. **1**, 686-693

20 Whittaker, M. M., Pan, H. Y., Yukl, E. T. and Whittaker, J. W. (2007) Burst kinetics and redox transformations of the active site manganese ion in oxalate oxidase: implications for the catalytic mechanism. J. Biol. Chem. **282**, 7011-7023

21 Escutia, M. R., Bowater, L., Edwards, A., Bottrill, A. R., Burrell, M. R., Polanco, R., Vicuña, R. and Bornemann, S. (2005) Cloning and sequencing of two *Ceriporiopsis subvermispora* bicupin oxalate oxidase allelic isoforms: implications for the reaction specificity of oxalate oxidases and decarboxylases. Appl. Environ. Microbiol. **71**, 3608-3616

22 Dutton, M. V. and Evans, C. S. (1996) Oxalate production by fungi: its role in pathogenicity and ecology in the soil environment. Can. J. Microbiol. **42**, 881-895

23 Dunwell, J. M., Khuri, S. and Gane, P. J. (2000) Microbial relatives of the seed storage proteins of higher plants: conservation of structure and diversification of function during evolution of the cupin superfamily. Microbiol. Mol. Biol. Rev. **64**, 153-179

24 Leslie, A. G. (2006) The integration of macromolecular diffraction data. Acta Crystallogr. Sect. D Biol. Crystallogr. **62**, 48-57

25 Evans, P. (2006) Scaling and assessment of data quality. Acta Crystallogr. Sect. D Biol. Crystallogr. **62**, 72-82

26 Collaborative Computational Project Number 4. (1994) The CCP4 suite: programs for protein crystallography. Acta Crystallogr. Sect. D Biol. Crystallogr. **50**, 760-763

27 Matthews, B. W. (1968) Solvent content of protein crystals. J. Mol. Biol. **33**, 491-497

28 Murshudov, G. N., Vagin, A. A. and Dodson, E. J. (1997) Refinement of macromolecular structures by the maximum-likelihood method. Acta Crystallogr. Sect. D Biol. Crystallogr. **53**, 240-255

29 Jones, T. A., Zou, J. Y., Cowan, S. W. and Kjeldgaard, M. (1991) Improved methods for building protein models in electron density maps and the location of errors in these models. Acta Crystallogr. Sect. D Biol. Crystallogr. **47**, 110-119

30 Emsley, P. and Cowtan, K. (2004) Coot: model-building tools for molecular graphics. Acta Crystallogr. Sect. D Biol. Crystallogr. **60**, 2126-2132

31 Read, R. J. (1986) Improved fourier coefficients for maps using phases from partial structures with errors. Acta Crystallogr. Sect. A **42**, 140-149

32 Guex, N. and Peitsch, M. C. (1997) SWISS-MODEL and the Swiss-PdbViewer: an environment for comparative protein modeling. Electrophoresis **18**, 2714-2723

33 Muthusamy, M., Burrell, M. R., Thorneley, R. N. F. and Bornemann, S. (2006) Real-time monitoring of the oxalate decarboxylase reaction and probing hydron exchange in the product, formate, using Fourier transform infrared spectroscopy. Biochemistry **45**, 10667-10673

34 Cruickshank, D. W. J. (1999) Remarks about protein structure precision. Acta Crystallogr. Sect. D Biol. Crystallogr. **55**, 583-601

35 Laskowski, R. A., Macarthur, M. W., Moss, D. S. and Thornton, J. M. (1993) PROCHECK: a program to check the stereochemical quality of protein structures. J. Appl. Crystallog. **26**, 283-291

Table 1 Summary of X-ray data and model parameters for oxalate decarboxylase mutants

Variant	R92A	E162A	Δ162-163	S161A
Data collection				
Radiation source	RU-H3RHB	RU-H3RHB	ESRF ID14-2	RU-H3RHB
Wavelength (Å)	1.542	1.542	0.933	1.542
Cell parameters (Å)	a = b = 154.5	a = b = 154.7	a = b = 154.9	a = b = 154.7
	c = 122.3	c = 122.1	c = 123.3	c = 121.9
Resolution range* (Å)	28.04 - 2.80	28.04 - 3.10	58.93 - 2.00	31.72 - 2.10
	(2.95 - 2.80)	(3.27 - 3.10)	(2.11 - 2.00)	(2.21 - 2.10)
Unique reflections	13947	10285	38270	32697
Completeness* (%)	99.9 (100.0)	99.5 (99.9)	99.9 (99.1)	99.9 (99.9)
Multiplicity	7.7 (7.6)	5.9 (5.9)	8.9 (7.0)	7.8 (7.3)
R_{merge}*†	0.156 (0.352)	0.152 (0.283)	0.098 (0.293)	0.140 (0.375)
$\langle I/\sigma(I)\rangle$*	13.4 (6.2)	9.8 (6.3)	22.2 (5.6)	15.3 (5.9)
Refinement				
R_{cryst}‡ (95% of data; %)	13.4	16.3	12.8	13.8
R_{free}‡ (5% of data; %)	21.1	21.9	16.6	18.3
DPI§ (based on R_{free}; Å)	0.297	0.383	0.103	0.130
Ramachandran plot‖ (%)	86.7	87.3	89.1	88.6
Rmsd bond distances (Å)	0.016	0.015	0.016	0.015
Rmsd bond angles (°)	1.612	1.504	1.499	1.438
Contents of model				
Protein residues	377	377	375	377
Water molecules	215	0	411	412
Manganese ions	2	2	2	2
Other ligands¶	-	-	1 x chloride	1 x formate
PDB accession code	2UY8	2UY9	2UYA	2UYB

* The figures in parentheses indicate the values for outer resolution shell.

† $R_{merge} = \sum_h \sum_l |I_{hl} - \langle I_h \rangle| / \sum_h \sum_l \langle I_h \rangle$, where I_l is the l^{th} observation of reflection h and $\langle I_h \rangle$ is the weighted average intensity for all observations l of reflection h.

‡ The R-factors R_{cryst} and R_{free} are calculated as follows: $R = \sum(|F_{obs} - F_{calc}|)/\sum|F_{obs}| \times 100$, where F_{obs} and F_{calc} are the observed and calculated structure factor amplitudes, respectively.

§ Diffraction-component precision index [34] – an estimate of the overall coordinate errors calculated in REFMAC5 [28].

‖ Residues with most favoured Φ/Ψangles as calculated using PROCHECK [35].

¶ Not including buffer or cryoprotectant molecules that are remote from the manganese sites.

Table 2 Activities of oxalate decarboxylase mutants prepared with the short heat shock protocol*

Site 1 or 2	Oxalate decarboxylase			Specific activity†	
Mutant	V_{max}†	K_m	k_{cat}/K_m†	Oxalate oxidase	Dye oxidation
	(U mg^{-1})	(mM)	(M^{-1} s^{-1})	(U mg^{-1})	
Wild type‡	21.0 ± 1.2 (100)	16.4 ± 3.4	950 ± 200 (100)	0.03 (100)	0.09 (100)
***1* R92A‡§**	0‖	–¶	–¶	0#	0.05 (56)
1 R92K‡	0.195 ± 0.008 (1)	1.9 ± 0.5	76 ± 20 (8)	0#	0.05 (56)
***1* E162A‡§**	0‖	–¶	–¶	0.02 (67)	0.11 (122)
1 E162Q‡	0.230 ± 0.014 (1)	13.5 ± 2.7	13 ± 3 (1)	0.03 (100)	0.21 (233)
***1* Δ162-3§**	0.213 ± 0.015 (1)	2.3 ± 0.9	69 ± 27 (7)	0.08 (247)	0.08 (91)
2 R270A‡	0.263 ± 0.010 (1)	8.0 ± 1.4	24 ± 4 (3)	0#	0.06 (67)
2 R270K‡	0.554 ± 0.018 (3)	1.14 ± 0.25	361 ± 80 (38)	0#	0.07 (78)
2 E333A‡	1.29 ± 0.05 (6)	4.1 ± 0.8	235 ± 50 (25)	0.02 (50)	0.03 (33)
2 E333Q‡	0‖	–¶	–¶	0#	0.06 (67)

* Recombinant oxalate decarboxylase enzymes were expressed in *E. coli* with a 2 min 42 ˚C heat shock prior to induction.

† Values in parentheses indicate percentage compared with wild type enzyme.

‡ Published previously [12], but original data have since been re-analysed to provide estimates of standard errors as described in the Experimental Procedures.

§ Mutants whose structures are described herein are highlighted in bold.

‖ Detection limit was 0.03 U mg^{-1}.

¶ –, not determined.

Detection limit was 0.01 U mg^{-1}.

Table 3 Activities of oxalate decarboxylase site 1 mutants prepared with the long heat shock protocol*

Site 1 or 2	Oxalate decarboxylase			Specific activity†	
Mutant	V_{max}†	K_m	k_{cat}/K_m†	Oxalate oxidase	Dye oxidation
	(U mg^{-1})	(mM)	(M^{-1} s^{-1})	(U mg^{-1})	
Wild type	94.9 ± 2.3 (100)	6.6 ± 0.6	10,670 ± 960 (100)	0.04 (100)	0.45 (100)
1 E162D	27.6 ± 1.9 (29)	17.4 ± 3.9	1,180 ± 280 (11)	0.02 (34)	0.04 (9)
2 E333D	0.85 ± 0.08 (1)	6.3 ± 2.3	101 ± 39 (1)	0.03 (67)	0.12 (26)
1 Δ162-4	0‡	–§	–§	0.12 (304)	0.06 (13)
1 T165P	2.90 ± 0.37 (3)	25 ± 9	85 ± 33 (1)	0.01 (20)	0.04 (8)
***1* S161A**‖	14.3 ± 1.3 (15)	71 ± 14	149 ± 32 (1)	≤0.01 (≤12)	0.03 (7)
1 S164A	13.8 ± 0.9 (15)	31 ± 5	332 ± 60 (3)	≤0.01 (≤12)	0.03 (7)
1 D297A	47.3 ± 2.5 (50)	11.2 ± 2.3	3,150 ± 660 (30)	0.12 (320)	0.40 (89)
1 H299A	46.3 ± 2.5 (49)	11.6 ± 2.2	2,960 ± 590 (28)	0.01 (31)	0.06 (14)

* Recombinant oxalate decarboxylase enzymes were expressed in *E. coli* with a 20 min 42 ˚C heat shock prior to induction.

† Values in parentheses indicate percentage compared with wild type enzyme.

‡ Detection limit was 0.03 U mg^{-1}.

§ –, not determined.

‖ Mutants whose structures are described herein are highlighted in bold.

Table 4 Manganese content of oxalate decarboxylase mutants

Site 1 or 2 Mutant	Mn/subunit
Wild type	1.2*, 1.2†, 1.3†
***1* R92A‡**	0.8[a]
1 R92K	0.9[a]
***1* E162A‡**	1.4[a]
1 E162Q	1.8[a]
2 R270K	0.7[a]
2 E333A	1.0[a]
2 E333Q	0.6[a]

* Recombinant enzyme was expressed in *E. coli* with a 2 min 42 ˚C heat shock prior to induction.

† Recombinant enzyme was expressed in *E. coli* with a 20 min 42 ˚C heat shock prior to induction.

‡ Mutants whose structures are described herein are highlighted in bold.

Scheme 1 Proposed divergent catalytic cycles of oxalate decarboxylase and oxalate oxidase

See the text for evidence for these cycles.

Figure 1 Structure of the wild type oxalate decarboxylase and superposition of site 2 mutant structures

A Figure showing the location of the OxdC subunit (shown in blue cartoon representation) within the context of the hexamer (depicted as a semitransparent grey surface). The magenta spheres represent the manganese ions at sites 1 and 2 (labelled in the enlarged view). The lid region (residues 160-166) is highlighted in red for the open (PDB code 1J58 [11]) and green for the closed (PDB code 1UW8 [12]) conformations. Access to site 1 is via the channel that runs through the centre of the hexamer. For comparison, the plant oxalate oxidase monomer structure (PDB code 1FI2 [16]) is also shown below (pale yellow cartoon) in the same relative orientation as the OxdC N-terminal domain, with the equivalent of the lid region highlighted in red (residues 158-160). **B** Stereoview showing key residues and waters around site 2 for all six known oxalate decarboxylase structures, where: green = wild type closed (PDB code 1UW8 [12]); grey = wild type open (PDB code 1J58 [11]); blue = R92A; orange = E162A; red = Δ162-3; and magenta = S161A. The dotted lines indicate interactions between the manganese, its protein ligands, and water molecules in the closed structure. The 'W' indicates the second water molecule that is only seen in the open structure. The figures were generated using PyMOL (http://www.pymol.org).

Figure 2 Structures of oxalate decarboxylase site 1 mutants

Stereoviews showing key residues and ligands (i.e. waters, formate or chloride) around site 1 and the lid region. In each case, the wild type open (PDB code 1J58 [11]) and closed (PDB code 1UW8 [12]) structures are shown for reference with carbons coloured grey and green respectively, and the mutant structures (R92A, E162A, Δ162-3 and S161A) are depicted with magenta carbons. The main chain backbone of the lid regions (residues 160-166 in oxalate decarboxylase) are shown in ribbon representation. The dotted lines indicate interactions between the manganese, its protein ligands, and water molecules in the closed structure. In the R92A mutant structure, 'W' indicates the water molecule that partially fills the space occupied by the guanidinium group of the wild type side chain. In the Δ162-3 mutant structure, a chloride ion is shown in yellow. The equivalent region of the plant oxalate oxidase is shown with orange carbons for comparison with the Δ162-3 mutant structure. In the S161A mutant, 'W' indicates the water molecule adjacent to Glu162, the formate and the Oγ of Thr165 (not shown) in this structure. Figures were generated using PyMOL (http://www.pymol.org).

Figure 3 X-band EPR anaerobic spectra of the R92A oxalate decarboxylase mutant in the presence of oxalate or formate

The anaerobic samples contained mutant protein (80 μM), 50 mM citrate, pH 4.0, 20% glycerol and 200 mM NaCl with either (a) no additive, (b) 200 mM formate or (c) 200 mM oxalate.

Biochemical Journal Immediate Publication. Published on 6 Aug 2007 as manuscript BJ20070708

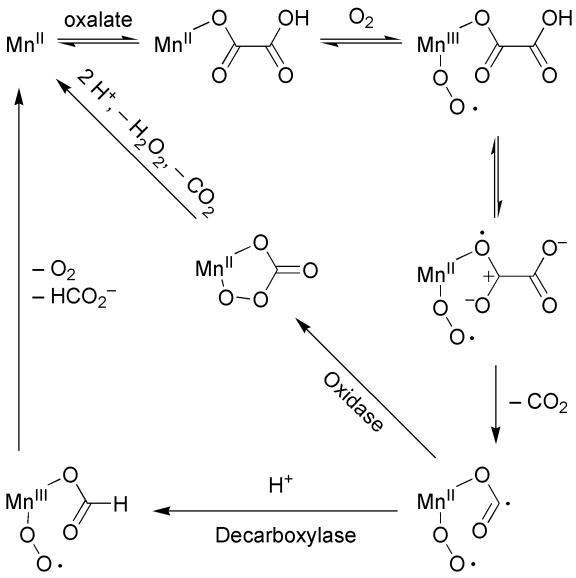

Biochemical Journal Immediate Publication. Published on 6 Aug 2007 as manuscript BJ20070708

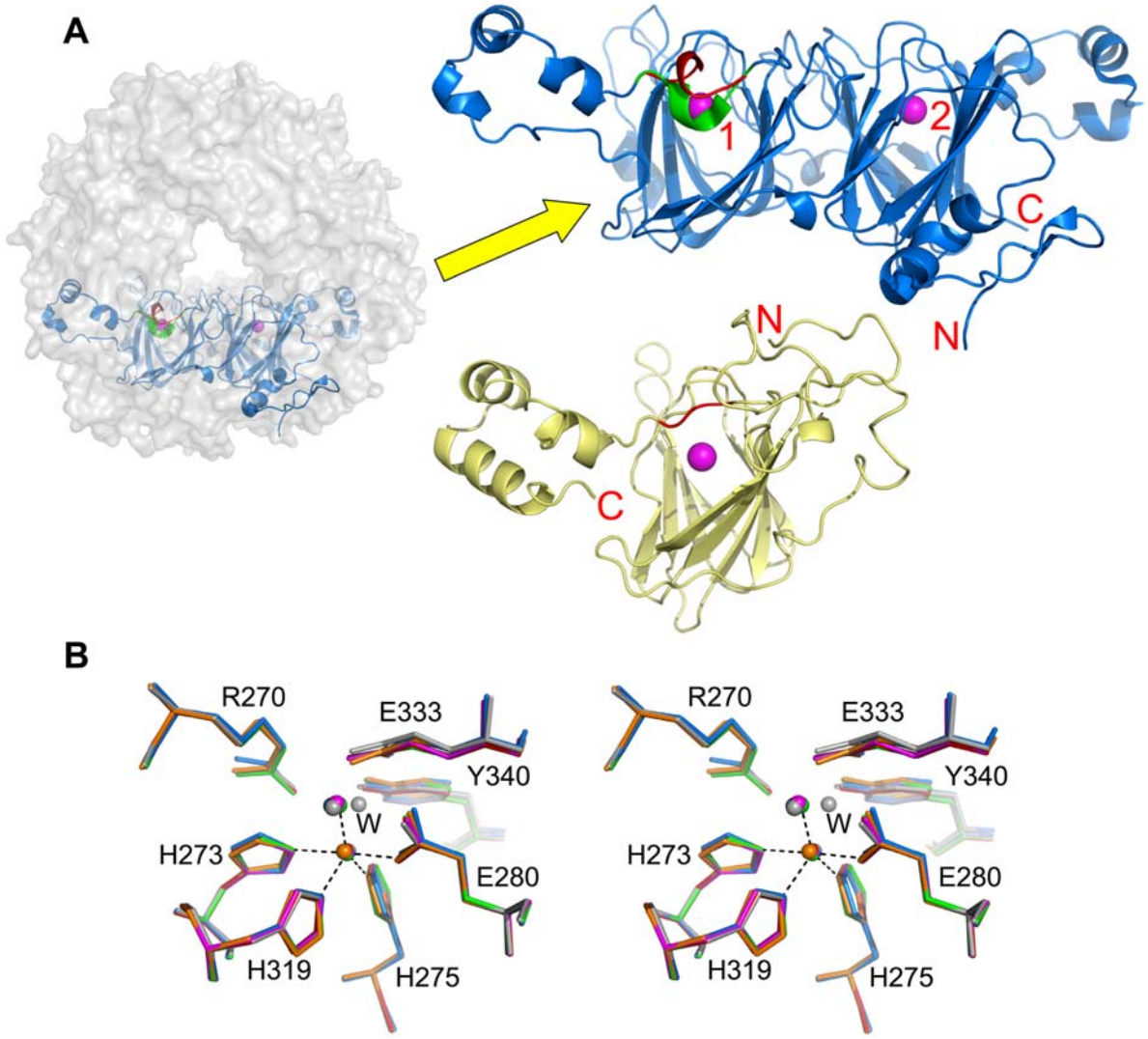

Biochemical Journal Immediate Publication. Published on 6 Aug 2007 as manuscript BJ20070708

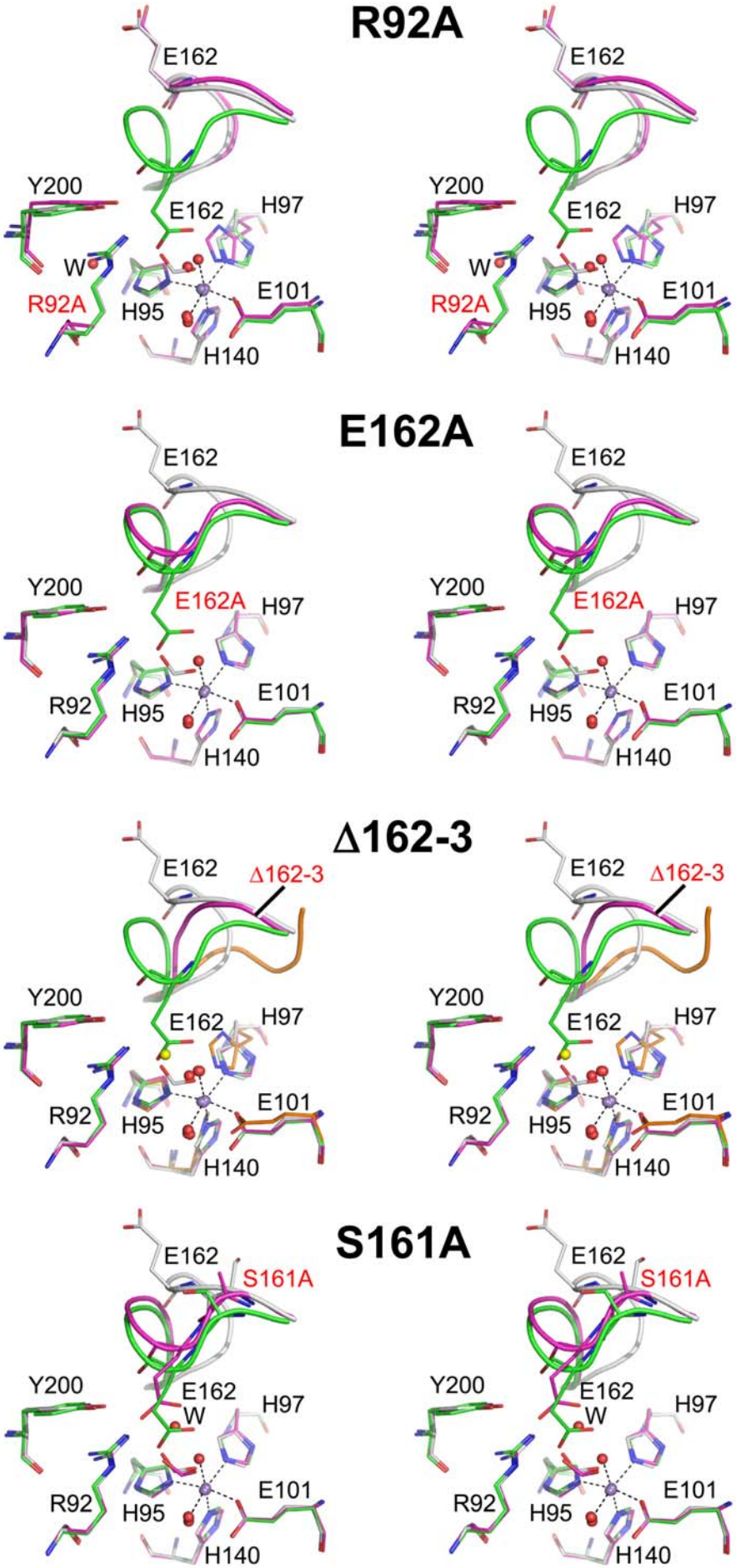

Biochemical Journal Immediate Publication. Published on 6 Aug 2007 as manuscript BJ20070708